Fast Response Aerodynamic Probe Measurements in a Turbulent Pipe Flow

Chr. Gossweiler, D. Herter, P. Kupferschmied

ETH Zürich, Switzerland

This paper describes the measurements with a fast response probe measurement system in a fully developed turbulent pipe flow.

The task of this experiment is to compare the fast response pressure probe results to hot wire data of the well known experiment of LAUFER 1954 and to verify the ability of the aerodynamic probe system to determine turbulence quantities.

The results presented cover the time averaged flow data and the turbulence quantities like intensities, shear stresses, probability densities, length scales and wave number spectra.

1. Introduction

The fast response probe measurement system is designed for measurements in highly turbulent turbomachine flows. The probe built for the present measurements has four piezoresistive miniature pressure transducers (Figure 1-1) and is of cylindrical shape with 2.5 mm external diameter.

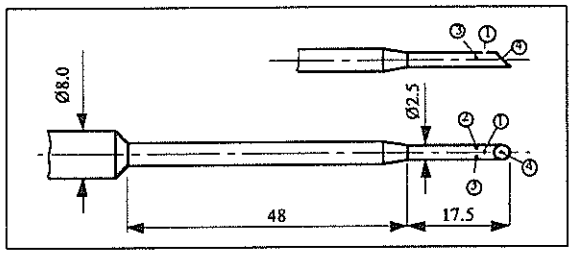

Figure 1-1 *Cylindrical pressure probe (Ø 2.5 mm) with four miniature pressure sensors*

The probe design, manufacture and calibration are described in GOSSWEILER / HUMM / KUPFERSCHMIED 1990. After the manufacture of the probe the sensors were statically and dynamically calibrated with respect to pressure and temperature. The static calibration data is used with a "model based reconstruction" technique to compensate for all systematic static errors of the sensor. This allows later quantification of the remaining static, random and the dynamic errors. After the aerodynamic calibration (KUPFERSCHMIED / GOSSWEILER 1992) the probe could be applied to measurements. The elements of the fast response measurement system are shown in figure 1-2.

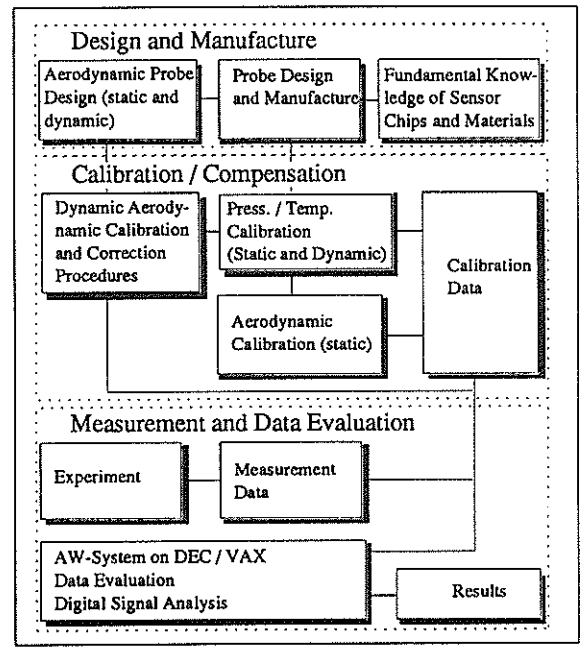

Figure 1-2 *Elements of the fast response probe measurement system*

2. Set-up of the pipe flow experiment

Figure 2-1 shows the schematic view of the pipe flow experiment, consisting of a filter, flow straightener, nozzle and the pipe with a roughened surface in the first part. The length L of the precision steel tube is 10.6 m with an inner diameter D of 200 mm. The maximum blockage of the probe is less than 2%.

The experiments with the fast response probe were carried out at a Mach number of Ma = 0.2 with a Reynolds number of Re_D = 800'000.

The signals of the fast response probe are amplified and collected with an eight channel 12 bit data acquisition system with a sampling rate of 100 kHz (figure 2-2).

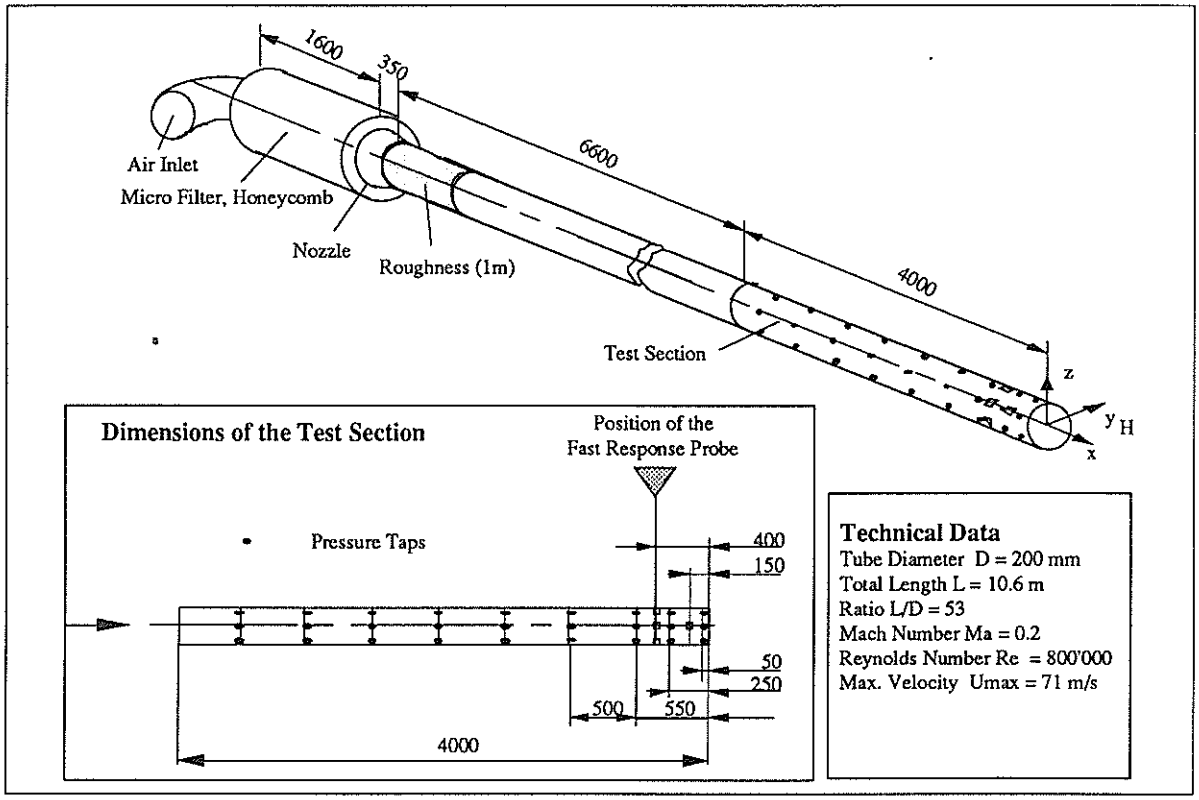

Figure 2-1 *Set-up of the pipe flow experiment*

The cut-off frequency of the antialiasing filters was set to 22 kHz. To obtain sufficient accuracy for statistical estimates 262'000 data points were collected at each traverse position.

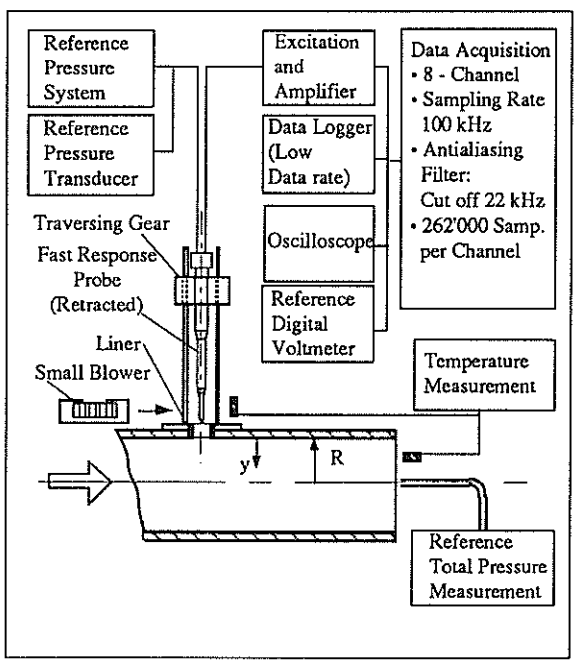

Figure 2-2 *Fast response probe set-up*

In order to examine the turbulent pipe flow, conventional wall pressure and Pitot tube measurements were taken. The wall static pressure shows a linear drop dp/dx in the test section ($33 \le x/D \le 53$) with deviations from linearity less than 0.15% of the maximum dynamic head. The wall shear stress $\tau_w = (R/2)\, dp/dx$ then becomes 7.66 N/m^2 for $Re_D = 800'000$.

By traversing a conventional Pitot tube at the outlet of the test section the normalized velocity profiles are obtained for $Re_D = 415'000$ (figure 2-3).

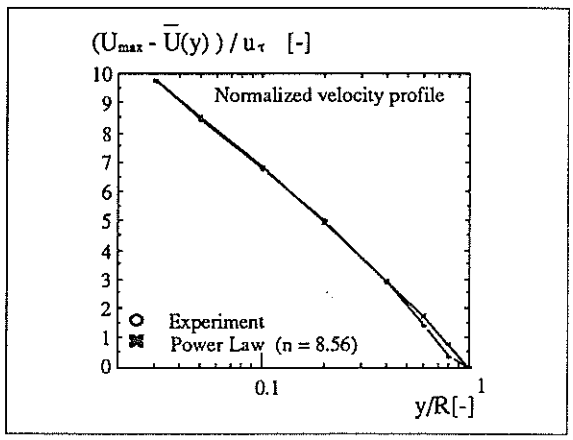

Figure 2-3 *Velocity profile (Re_D = 415'000)*

Compared to the power law of turbulent pipe flow with an exponent of n = 8.56 (Re_D = 415'000) the velocity

profiles show acceptable accuracy and symmetry (figure 2-4).

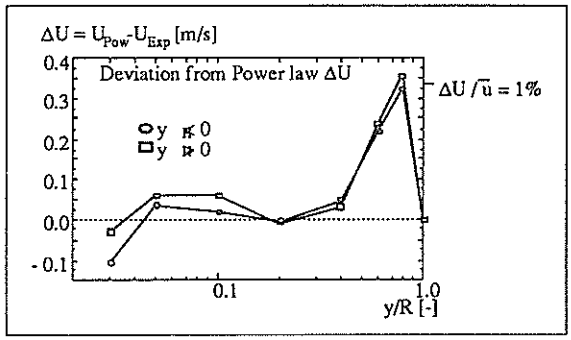

Figure 2-4 *Deviation from power law of turbulent pipe flow ($n = 8.56$, $Re_D = 415000$)*

3. Evaluation of the fast response data

To evaluate the large time series of the fast response probe the interactive data evaluation and signal analysis environment **AW-System** is used (HERTER / CHRISANDER / GOSSWEILER 1992). An overview of the data evaluation and signal analysis steps needed is given in figure 3-1 (see next page).

1) Conversion of the sensor signals into indicated pressures $\hat{p}_i$ and temperatures $\hat{T}_i$ using the static sensor calibration data. An example of the time history ($\Delta t = 0.01$ seconds) of the indicated pressures is given in figure 3-2. Since the indicated pressures are expressed with respect to the mean static pressure, sensor 1 indicates approximately the dynamic head. The indicated pressures of the sensors 2 and 3 are close to the true static pressure.

2) With the indicated pressures the indicated flow quantities defined in the spherical probe coordinate system are determined using the (static!) aerodynamic calibration data (KUPFERSCHMIED / GOSSWEILER 1992); figure 3-3.

3) Looking at the normalized autospectral densities of the indicated flow quantities an interference peak of the Kármán vortices downstream of the probe is visible in the yaw angle spectrum (figure 3-4). The signal powers of the interference peak and the yaw angle fluctuation of the flow are of the same order. The Strouhal number of the probe is $Str = f\ D_s / \overline{U} = 0.183$ and thus in good agreement with the measurements of OKAMOTO / YAGITA 1973. Since the interference of the Kármán vortices is mainly a systematic phenomenon with only a small bandwith it can be corrected with a specially designed inverse digital filter. The filter is designed according to the algorithm of MCCLELLAN / PARKS / RABINER 1979. For each traverse position a new set of filter coefficients has to be calculated.

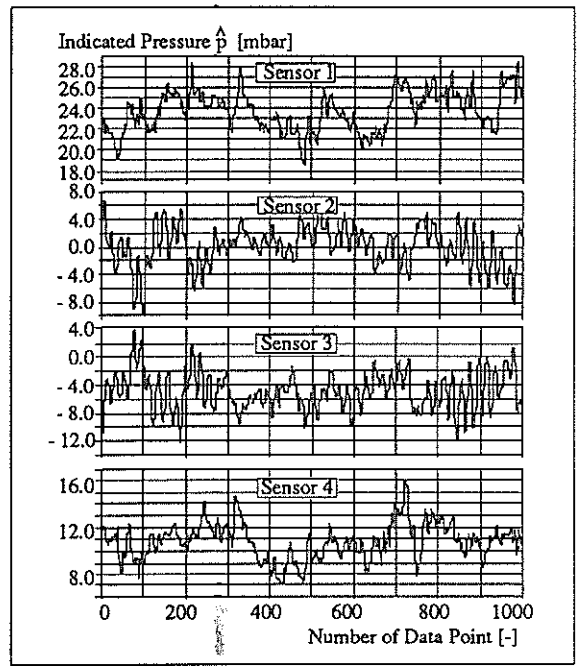

Figure 3-2 *Indicated pressures (10 ms duration); relative wall distance y/R = 0.5*

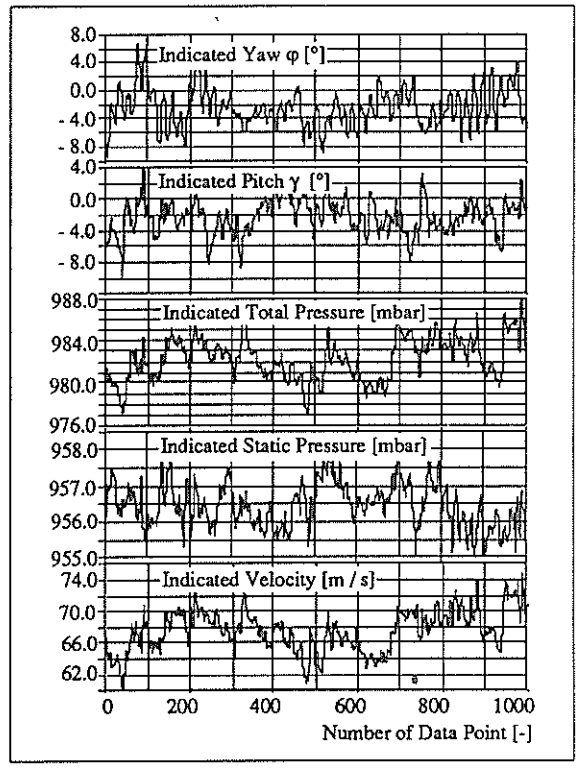

Figure 3-3 *Indicated flow quantities measured at a relative wall distance y/R = 0.5*

As an example for one radial position the gain factor of the transfer function $|H(j\omega)|$ is given in figure 3-5.

The effect of the correction on the yaw angle spectra is shown in figure 3-6.

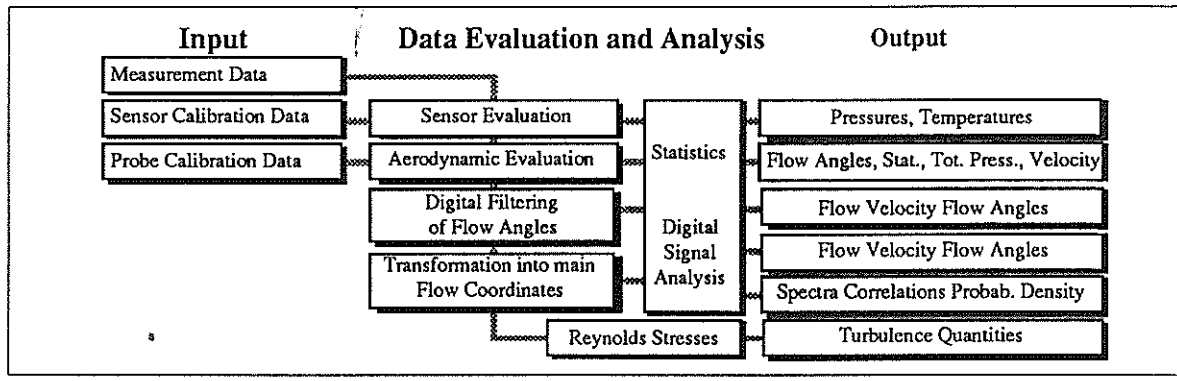

Figure 3-1 *Structure of the evaluation of the fast response data from the pipe flow experiment*

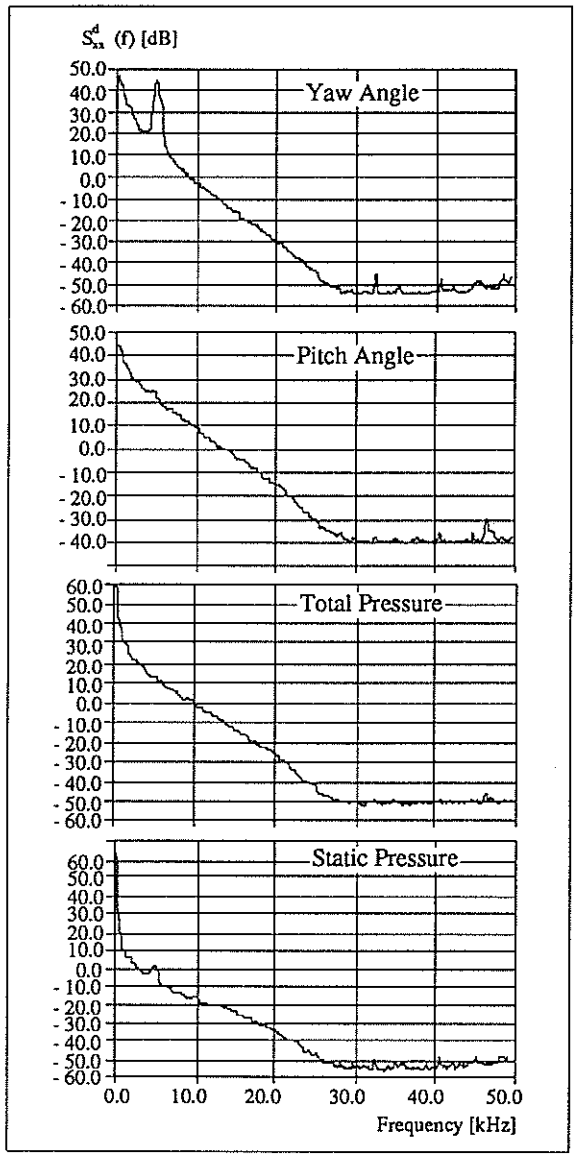

Figure 3-4 *Normalized spectral densities of the indicated flow quantities. In the yaw spectrum the interference peak of the Kârmân vortices is visible at about 5 kHz*

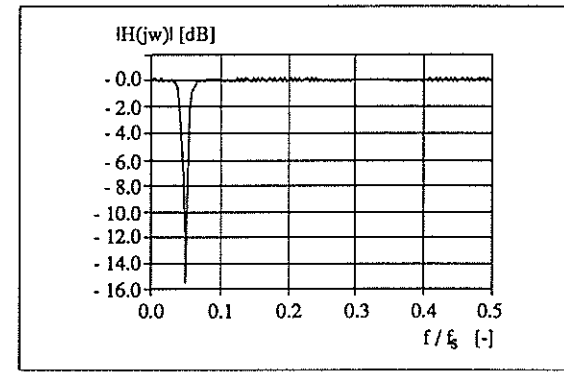

Figure 3-5 *Transfer function of an inverse digital filter for yaw angle correction. (frequency normalized with sampling frequency f_S)*

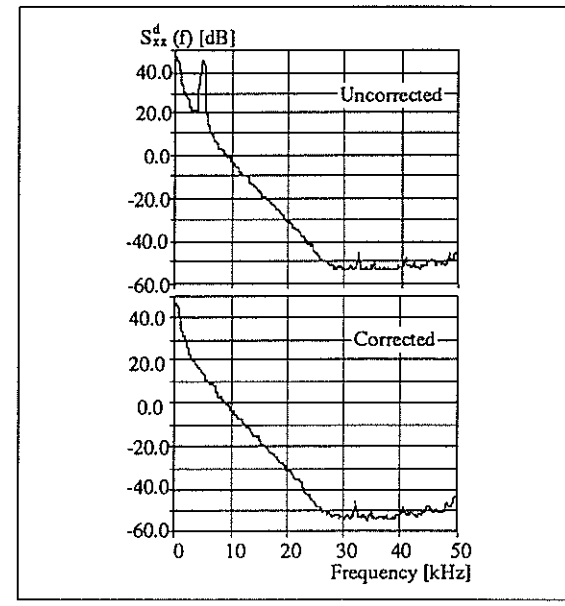

Figure 3-6 *Comparison of yaw angle spectra before and after correction*

4) The corrected flow quantities are transformed into cartesian main stream coordinate components U(t), V(t), W(t). The V and W components represent the radial and tangential components of the pipe flow vector.

4 Results of the fast response measurements

In this section the results of the fast response measurements are discussed and compared to the hot wire data of LAUFER 1954. In a first section the accuracy of the time averaged flow quantities is shown. In the following sections turbulence quantities like variance, normal and shear stresse, probability density, length scales and wave number spectra are presented.

4.1 Determination of time averaged flow quantities

After the adjustment of the sensors' zero and span the typical static errors of the pressure measurements are less than 20 Pa which is excellent for DC measurements with miniature sensors. Without adjustments the typical static errors of the temperature measurements (performed with the same pressure sensors; GOSSWEILER / HUMM / KUPFERSCHMIED 1990) arise to 1°C which is small enough for an accurate determination of the gas density.

The time averaged velocity with simple aerodynamic corrections for shaft influence and blockage is shown in figure 4-1.

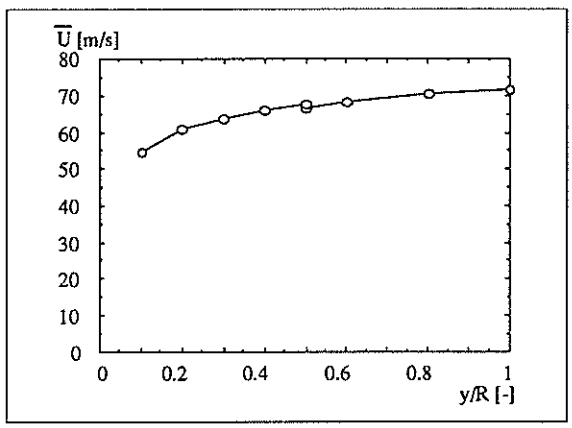

Figure 4-1 *Time averaged velocity $\overline{U}$ Maximal averaged velocity $\overline{U}_{max}$ = 71.7 m/s*

In comparison to the power law of turbulent pipe flow with n = 8.9 (Re_D = 800'000) the maximal deviations of the fast response measurements are ± 1.5 m/s (≈± 2% of $\overline{U}_{max}$). It must be pointed out that the accuracy could be increased by more careful aerodynamic corrections.

4.2 Variances, normal and shear stresses

The standard deviations of indicated yaw and pitch angle fluctuations are shown in figure 4-2. The standard deviation of the pitch angle fluctuations has a maximum value of 4.7° and systematically higher than for the yaw (a fact that will be discussed later).

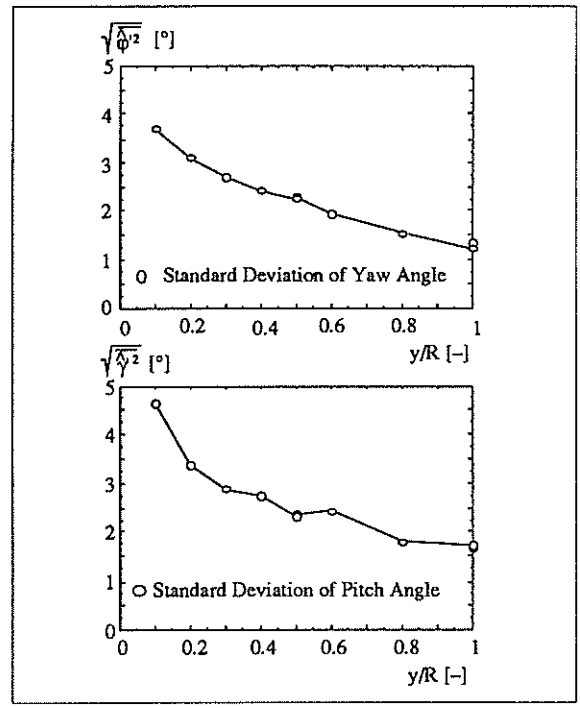

Figure 4-2 *Standard deviations of yaw and pitch angle fluctuations*

The standard deviation of the static pressure fluctuation is less than 1 mbar (3.7% of the maximum dynamic head). The standard deviation of the total pressure fluctuation increases with decreasing wall distance and is at maximum 3.1 mbar (12% of max. dyn. head) at a relative wall distance of y/R = 0.1 (figure 4-3).

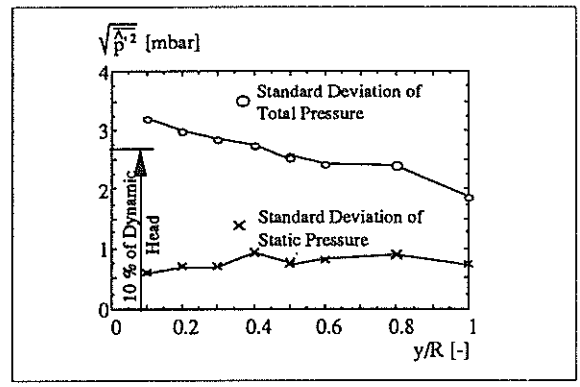

Figure 4-3 *Standard deviations of static and total pressure fluctuations*

Using the velocities U(t), V(t), W(t) defined in the main stream coordinate system the Reynolds stresses can be calculated and the relative turbulence intensities (non dimensional normal stresses) compared to the hot wire data of LAUFER 1954 (figure 4-4).

The turbulence intensity of the U component is slightly too high at the pipe center (at maximum 18%). The relative intensity of the radial component V is systematically too high at maximum 45% at y/R = 0.1. The turbulence intensity of the U component is mainly

influenced by the pitch angle fluctuations (figure 4-2). We assume that dynamic aerodynamic errors (HUMM / VERDEGAAL 1992)[1] of the pitch angle measurement lead to this systematically too high turbulence intensity of the V component. The turbulence intensity of the tangential component W is too low compared to LAUFER's data (at maximum 22% at y/R = 1).

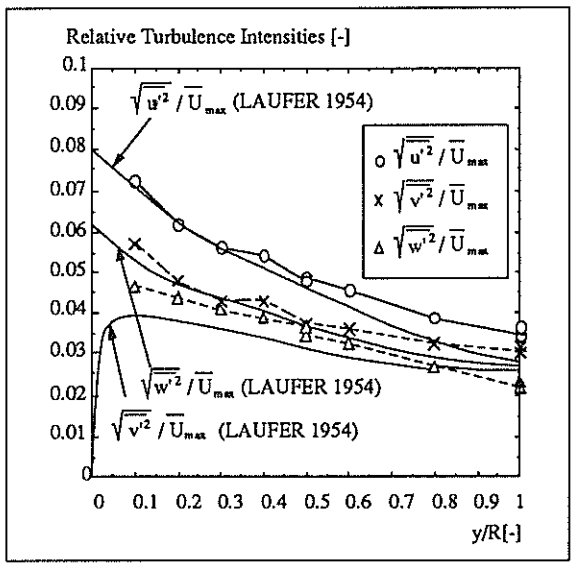

Figure 4-4 *Relative turbulence intensities as a function of the relative radius $Re_D = 800'000$*

The normalized shear stress $u'v'/u^2\tau$ is systematically far too low compared to the theoretical value. This is probably due to dynamic aerodynamic errors of the pitch angle measurement which lead to a bad correlation of the two components (figure 4-5). This will require further attention.

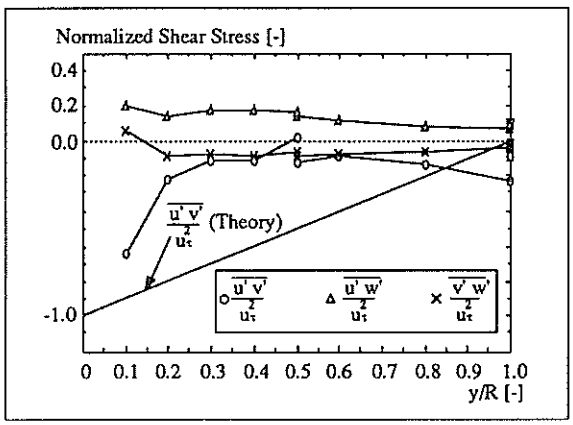

Figure 4-5 *Normalized shear stresses*

The normalized shear stresses $u'w'/u^2\tau$ and $v'w'/u^2\tau$ are near zero as expected.

[1] Dynamic aerodynamic errors of the flow angle measurements are described in HUMM / VERDEGAAL 1992. These errors can seriously affect the accuracy of fast response probe measurements.

4.3 Probability densities

The probability density distributions (pdd) of the flow angles are similar to Gaussian distributions due to little skewness and excess (figure 4-6).

The pdd of UV at y/R = 0.1 is shown in figure 4-7.

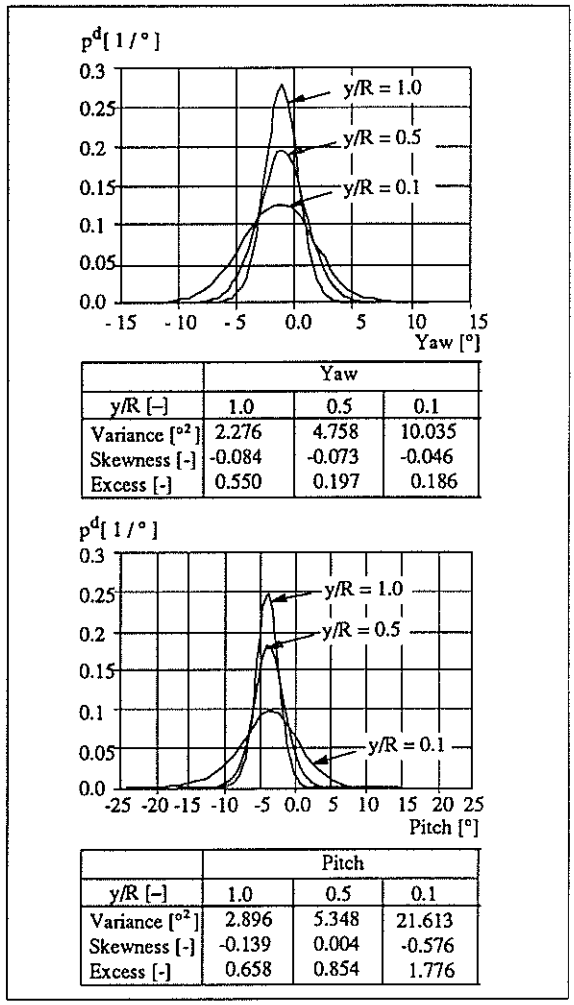

	Yaw		
y/R [–]	1.0	0.5	0.1
Variance [°²]	2.276	4.758	10.035
Skewness [-]	-0.084	-0.073	-0.046
Excess [-]	0.550	0.197	0.186

	Pitch		
y/R [–]	1.0	0.5	0.1
Variance [°²]	2.896	5.348	21.613
Skewness [-]	-0.139	0.004	-0.576
Excess [-]	0.658	0.854	1.776

Figure 4-6 *Probability densities of flow angle*

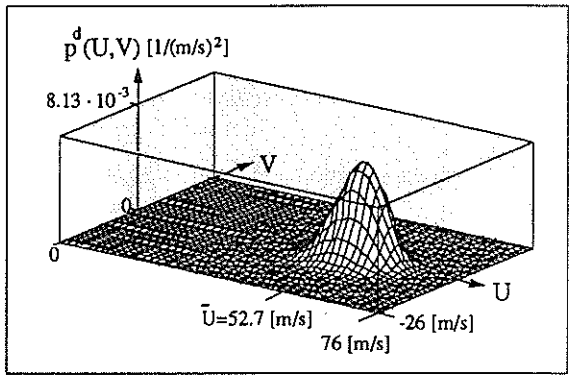

Figure 4-7 *Joint probability density of UV*

The probability for the flow vector to be in a certain angular range (denoted as cone angle by BROWNE et

al. 1989) can be calculated by integrating $p^d(\varphi)$, $p^d(\gamma)$ or by integrating $p_d(U,V)$ over a certain angular range α (figure 4–7).

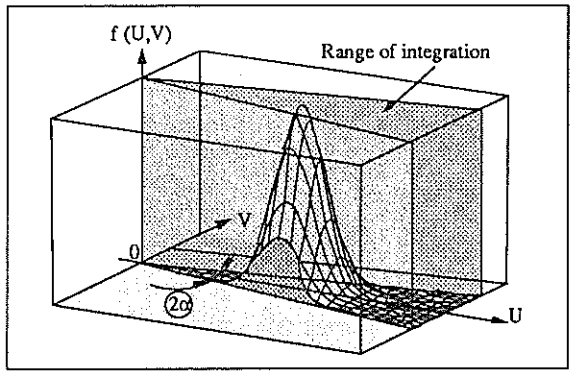

Figure 4-8 *Range of integration of $p^d(U,V)$*

By assuming Gaussian distributions for u' and v' the cone angle can also be calculated from the variances of u' and v':

$$p(\alpha,\overline{u'^2},\overline{v'^2}) = \frac{1}{\pi\sqrt{\overline{u'^2}\,\overline{v'^2}}} \int_0^{U_{max}} \int_0^{U\tan\alpha} e^{-\frac{1}{2}\left[\frac{(U-\overline{U})^2}{\overline{u'^2}} + \frac{v^2}{\overline{v'^2}}\right]} dV dU$$

The comparison of the cone angles thus obtained and those derived from the angle measurement show a reasonable agreement (figure 4-9). This indicates that the angle fluctuations were symmetric and of near Gaussian type.

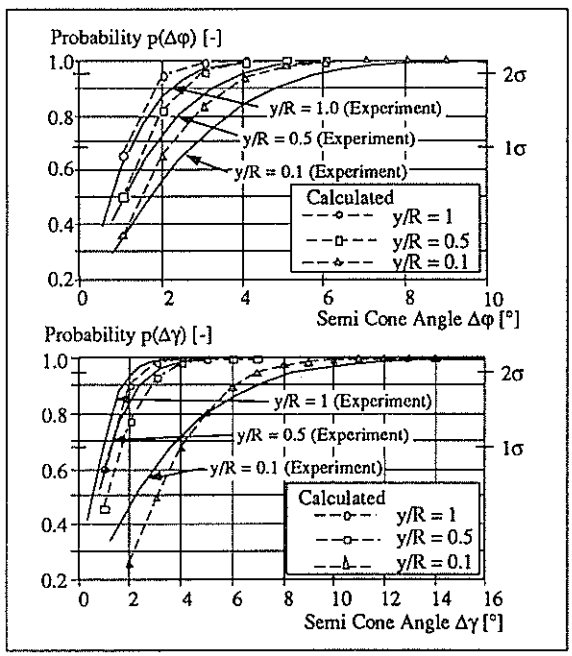

Figure 4-9 *Probability for the flow vector to be in a certain angular range (cone angle)*

Note that the angular range of the fast response probe (unstalled range, see HUMM / VERDEGAAL 1992) should be large enough to allow measurements in a turbulent flow. For example in the case of the pipe flow experiment for the pitch angle γ at a relative wall distance of 0.1 with only about 8% turbulence level (figure 4-4 for u' [2]) more than 3% of the measured points show cone angles higher than 10° (figure 4-9).

4.4 Length scales, turbulent dissipation

Under the Taylor hypothesis $\partial/\partial t = -U\,\partial/\partial x$ the length scales can be calculated. By integrating the estimate of the autocorrelation function $r_{u'u'}(\tau)$ (figure 4-10) the integral length scale[1] L can be determined (figure 4-11):

$$L = \overline{U} \int_0^{\infty} r_{u'u'}(\tau)\, d\tau$$

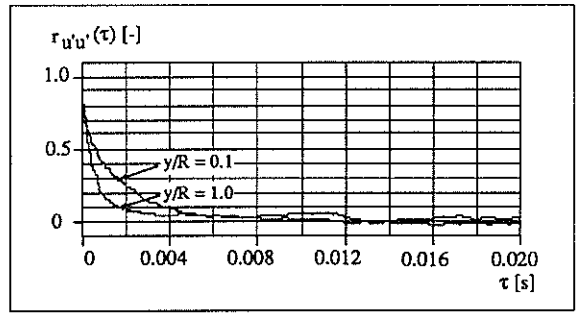

Figure 4-10 *Estimate of the autocorrelation. (determined with convolution and not via FFT to enhance the accuracy)*

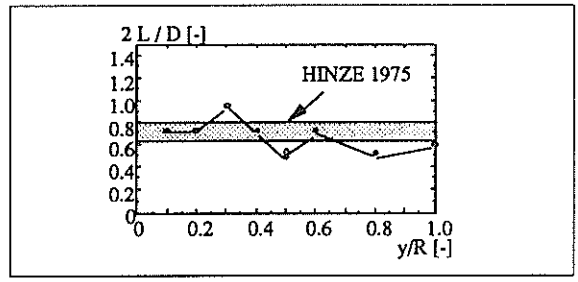

Figure 4-11 *Normalized integral length scale as a function of relative wall distance*

Comparing the integral length scales with the values given by HINZE 1975 (L is roughly 0.8 D/2) the results of the fast response probe show acceptable accuracy.

The Taylor-microscale λ can be determined using a parabola fit of the origin of the autocorrelation which is an even function. A good approximation of the Taylor scale is[2]:

$$\lambda \approx \frac{1}{\sqrt{2}} \tau_e \overline{U}$$

where τ_e represents the intersection of the parabola with the abscissa.

---

[1] Definitions see HEINIGER 1990; HINZE 1975; TENNEKES / LUMLEY 1972; BRADSHAW 1971; REYNOLDS 1974

[2] HEINIGER 1990

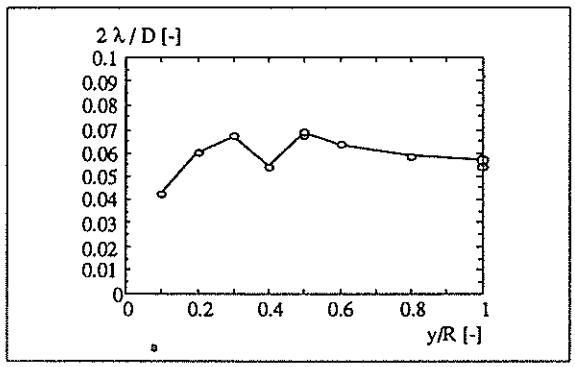

Figure 4-12 *Taylor-microscale*

A comparison with measurements by LAWN 1971 (Re_D = 90'000) shows that the fast response microscales are systematically too large. At y/R = 0.35 LAWN obtains maximum values of about $2\lambda/d = 0.045$ with a decrease to the wall (y/R = 0).

The turbulent dissipation can be approximated by:

$$\varepsilon \approx 15\,\nu\,\frac{\overline{u'^2}}{\lambda^2}$$

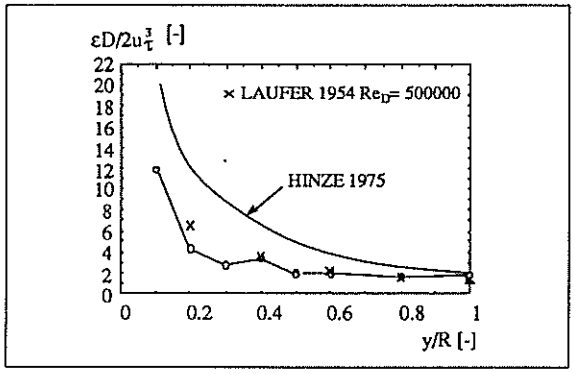

Figure 4-13 *Normalized turbulent dissipation*

The dissipation measured with the fast response system is comparable to the hot wire data of LAUFER measured at a Reynolds number of 500'000. HINZE 1975 suggests that the LAUFER values are too low and estimates the correct value from results obtained at a lower Reynolds number. Thus the values of the fast response system are too low but it must be pointed out that the measurement of the turbulent dissipation at high Reynolds numbers is extremely difficult.

4.5 Wave number spectra

The power spectral densities S^d_{xx} are normalized as wave number spectra (wave number $k = 2\pi f / \overline{U}$):

$$S^d_{u'u'}\left(k\frac{D}{2}\right) = \frac{1}{u'^2}\int_0^{f_u/2} S^d_{u'u'}(f)\,\frac{\overline{U}}{\pi D}\,df = 1$$

The wave number spectra of U, V, W at relative radii of y/R = 1.0 and y/R = 0.1, compared to the measurements of LAWN 1971 (Re_D = 90'000) are given in figures 4-14 and 4-15.

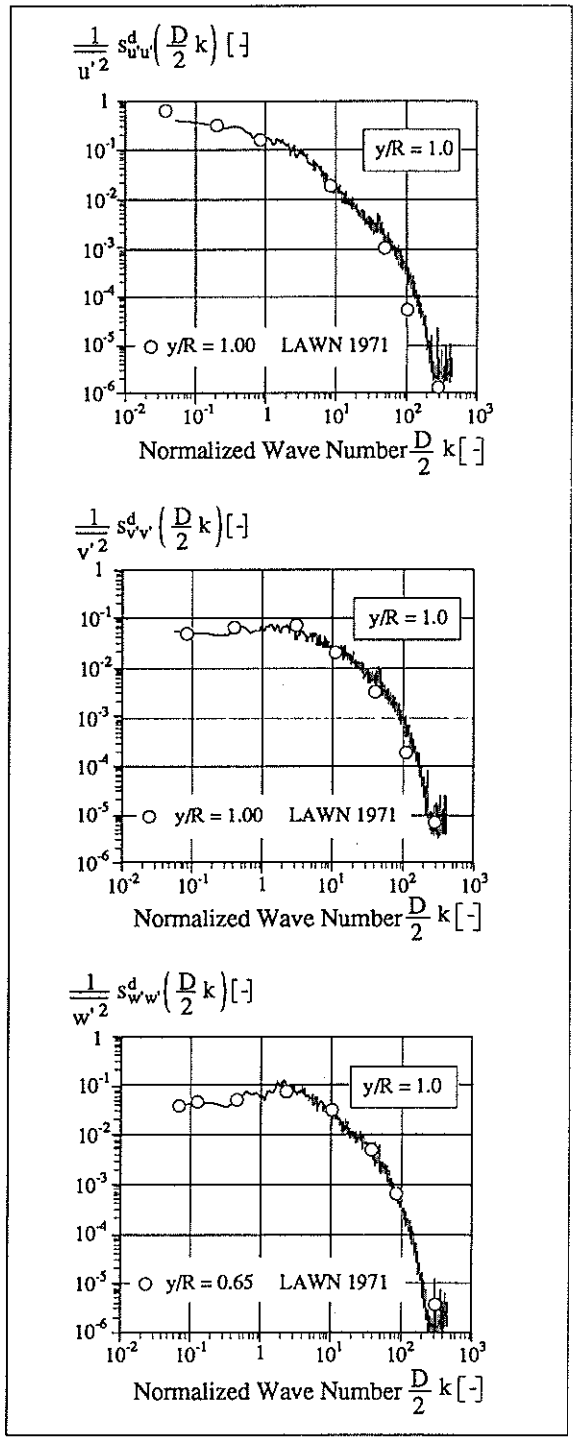

Figure 4-14 *Wave number spectra at y/R = 1.0 (pipe center)*

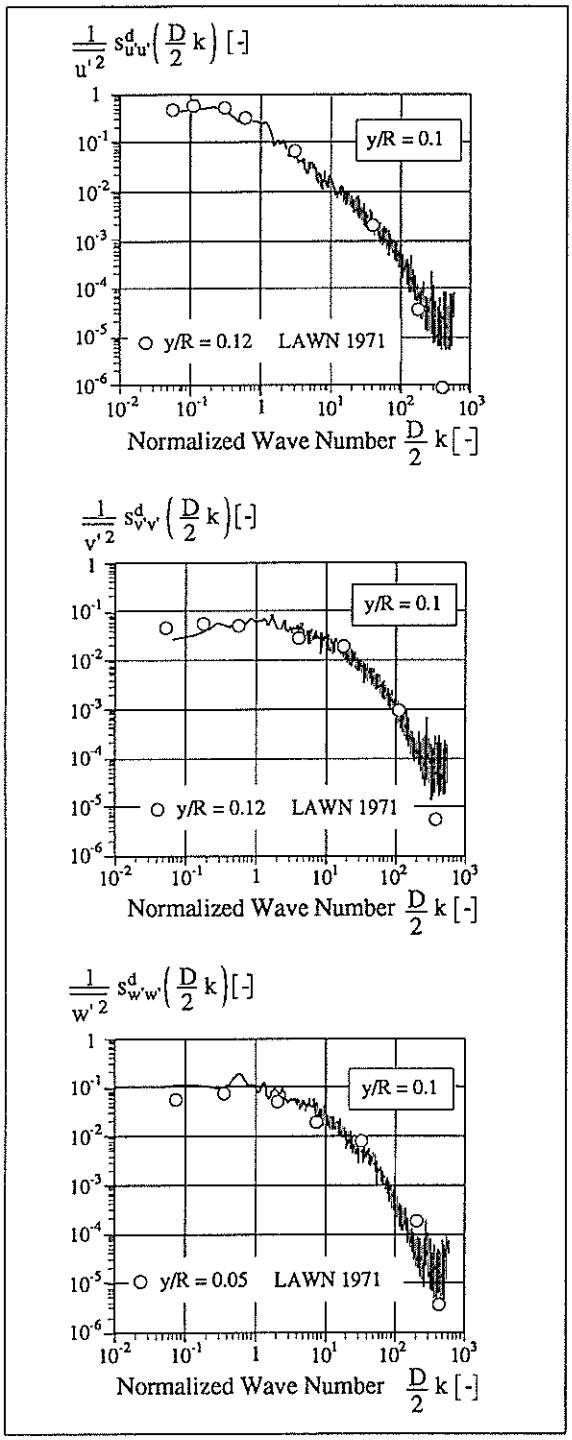

Figure 4-15 *Wave number spectra at y/R = 0.1 (near wall)*

The normalized wave number spectra show a fairly good agreement with the hot wire data of LAWN 1971.

5. Conclusions

Although the Mach number was low (Ma = 0.2), was quite accurate for a fast response probe system. This shows that the the static and dynamic signal components were reliably measured and evaluated.

The turbulence intensities of the U and W component show maximum deviations of 22% compared to the hot wire data of LAUFER 1954.

The turbulence intensity of the V component and the u'v' shear stress show large deviations from the expected values, probably due to dynamic aerodynamic errors of the pitch angle measurement. This aspect needs further improvement.

The length scales can be determined with acceptable accuracy with maximum systematic errors of 30%.

The high signal to noise ratio and the large bandwidth of the fast response probe measurement system promises to gain new insight into turbulent flows.

6. Acknowledgements

This work is supported by the Swiss National Science Foundation. The authors wish to thank C. Reshef for his support concerning the electronic equipment and H. Richner, P. Lehner and T. Künzli for their technical assistance.

7. Nomenclature

C	velocity (spherical probe coordinates) [m/s]
D	tube diameter [m]
D_S	diameter of cylindrical probe [m]
f	frequency [Hz]
f_s	sampling frequency [Hz]
$\|H(j\omega)\|$	gain of transfer function [-]
k	wave number [1/m]
L	length; integral length scale [m]
Ma	Mach number [-]
n	exponent of power law of pipe flow [-]
Re_D	Reynolds number [-]
p	pressure [mbar] [Pa]
p	probability [-]
$p^d(x)$	probability density [1/x]
$p^d(x,y)$	joint probability density [1/(xy)]
R	tube radius [m]
$r_{u'u'}(\tau)$	autocorrelation of u' [-]
S^d_{xx}	spectral density (power spectrum) [x^2] [dB]
Str	Strouhal number [-]
T	temperature [°] [K]
t	time [s]
U(t)	axial component of flow velocity [m/s]
$\overline{U}_{max}$	max. time averaged velocity in pipe flow [m/s]
u_τ	wall friction velocity [m/s]
u'(t)	turbulent fluctuation of U [m/s]
$\overline{u}$	mass averaged velocity of pipe flow [m/s]
$\overline{u'v'}$	shear stress of UV (covariance of U,V) [$(m/s)^2$]

$V(t)$	radial component of flow velocity [m/s]
$W(t)$	tangential component of flow velocity [m/s]
$\overline{x'^2}$	variance of x [x^2]
$\sqrt{\overline{x'^2}}$	standard deviation of x [x]
y	wall distance [m]
α	angle [°]
ε	dissipation per unit mass [m^2/s^3]
γ	pitch angle [°]
φ	yaw angle [°]
λ	Taylor-microscale [m]
π	3.14159...
σ	expected value of the standard deviation
τ	time lag of autocorrelation [s]
τ_e	intersection of parabola fit [s]
τ_w	wall shear stress [N/m^2]

Superscripts

'	turbulent fluctuation
^	indicated
¯	time-average

8. References

BROWNE L. W. B.; ANTONIA R. A.; CHUA L. P.
Velocity Vector Cone Angle in Turbulent Flows
Experiments in Fluids 8, 13-16 1989

GOSSWEILER C.; HUMM H.; KUPFERSCHMIED P.
The Use of Piezo Resistive Semi-Conductor Pressure Transducers for Fast Response Probe Measurements in Turbomachinery
Xth Symposium on Measuring Techniques for Transonic and Supersonic Flows in Cascades and Turbomachines, Bruxelles, 1990.

GOSSWEILER C.; HUMM H.; KUPFERSCHMIED P.
Dynamic Calibration of Piezoresistive Pressure Transducers in the Frequency Range of over 500 kHz
Micromechanics Europe, Berlin 1990.

KUPFERSCHMIED P.; GOSSWEILER C.
Calibration, Modeling and Data Evaluation Procedures for Aerodynamic Multihole Pressure Probe Measurements on the Example of a Four Hole Probe
XIth Symposium on Measuring Techniques for Transonic and Supersonic Flows in Cascades and Turbomachines, München, 1992.

HERTER D.; CHRISANDER N.; GOSSWEILER C.
AW-System - An Interactive Environment for the Evaluation of Large Time Series
XIth Symposium on Measuring Techniques for Transonic and Supersonic Flows in Cascades and Turbomachines, München, 1992.

HEINIGER K. CH.
Investigation of the Energy Stratification in Curved Cannel Flows (in German:Untersuchung über die Energieschichtung in turbulenter Strömung durch einen gekrümmten Kanal)
PhD thesis, ETH Nr. 9344, 1990

HINZE J. O.
Turbulence
Mac Graw Hill 1975

HUMM, H.J.; VERDEGAAL J.I.
Aerodynamic Design Criteria for Fast Response Probes
XIth Symposium on Measuring Techniques for Transonic and Supersonic Flows in Cascades and Turbomachines, München, 1992.

LAUFER J.
The Structure of Turbulence in Fully Developed Pipe Flow
Nat. Advisory Comm. Aeronaut. Tech. Rep. No 1174, 1954, Updata 1975

LAWN C. J.
The Determination of the Rate of Dissipation in Turbulent Pipe Flows
J. Fluid Mech. 48; p 477-505; 1971

MCCLELLAN J. H.; PARKS T. W.; RABINER L. R.
FIR Linear Phase Filter Design Program
Programs for the Digital Signal Processing IEEE Press 1979

OKAMOTO T.; YAGITA M.
The Experimental Investigation on the Flow Past a Circular Cylinder of Finite Length Placed Normal to the Plane Surface
JSME Bulletin Vol 16 No 95 May 1973

REYNOLDS A. J.
Turbulent Flows in Engineering
John Wiley + Sons 1974

TENNEKES H.; LUMLEY J.L.
A First Course in Turbulence
MIT Press 1972 (Tenth Printing Ass)